


## Parity-violating contributions to nuclear spin-rotation interactions and to NMR shielding constants in tetrahedral molecules

I. Agustín Aucar \*

*Instituto de Modelado e Innovación Tecnológica, CONICET, and Departamento de Física,  
Facultad de Ciencias Exactas y Naturales, UNNE, Avenida Libertad 5460, W3404AAS Corrientes, Argentina*

Yuly Chamorro  and Anastasia Borschevsky 

*Faculty of Science and Engineering, Van Swinderen Institute for Particle Physics and Gravity,  
University of Groningen, 9747 AG Groningen, Netherlands*



(Received 10 August 2022; accepted 28 October 2022; published 1 December 2022)

In natural processes involving weak interactions, a violation of spatial parity conservation should appear. Although the parity-violation effects are expected to be observable in molecular systems, their tiny magnitude has prevented their detection to date. We present a theoretical analysis of four-component relativistic nuclear-spin-dependent parity-violating nuclear spin-rotation and NMR shielding tensors in a set of tetrahedral chiral molecules. This work emphasizes the significant contribution of the ligands and the electronic structure of the chiral center in enhancing these effects, paving the way for the targeted design of promising molecules for measurements.

DOI: [10.1103/PhysRevA.106.062802](https://doi.org/10.1103/PhysRevA.106.062802)

### I. INTRODUCTION

The parity-nonconserving nature of physical phenomena affected by weak interactions is known to be responsible for asymmetric processes with respect to spatial inversion of the coordinates of the particles in a system. The existence of parity violation (PV) was first postulated by Lee and Yang [1], and it was Wu *et al.* [2] who provided its pioneering experimental verification using  $^{60}\text{Co}$  nuclei and observing nuclear  $\beta$ -decay processes due to weak interactions. While the first confirmations of the existence of PV effects were carried out in nuclear systems [2,3], since then these phenomena have been observed also in atoms [4–11].

Parity-violation effects due to the weak interactions between electrons and nucleons are expected to be observable even in molecular systems. These effects, for instance, are predicted to result in a small energy difference between a chiral molecule's two enantiomers. This happens as a result of the PV interactions mixing states with the opposite parity, which causes the chiral molecules to undergo a first-order energy shift [12]. High-resolution spectroscopy has been used to look for these energy shifts between different states of two chiral enantiomers since this phenomenon was identified, but so far no unambiguous detection of them has been made in this way. The observation of PV effects in chiral molecules using various techniques, such as electronic, vibrational, Mössbauer, and nuclear magnetic resonance (NMR) spectroscopy, as well as measurements of the time dependence of optical activity, has been the subject of numerous additional complementary experimental routes over the past five decades

[12–21]. Although PV effects in molecules have a strong theoretical foundation and a significant potential impact, they have never been clearly identified experimentally.

Alongside the new experimental capabilities, reliable theoretical studies are crucial for the success of such ambitious measurements at all of their stages, from selecting optimal molecules, through planning of the experimental procedure, to the interpretation of the results. In particular, several theoretical studies addressed the influence of PV effects on NMR parameters like shielding or indirect spin-spin coupling tensors in molecular systems [22–32], and the first such measurements were recently attempted by Eills *et al.* [33] and also by Blanchard *et al.* [34]. In their works, some proof-of-principle investigations based on new experimental techniques using NMR spectroscopy were presented to search for PV effects in molecular systems. This type of study could be decisive in taking a step forward in the use of high-precision experiments to detect these parity-nonconserving interactions in molecules for the first time [35].

In this work we concentrate on the nuclear spin-rotation (NSR) tensor, a property measured in microwave spectroscopy, where molecular PV effects are predicted to be observed by comparing the measurements of this parameter in two enantiomers of a chiral molecule. When the nuclear-spin-dependent (NSD) PV Hamiltonian is considered, a difference between the NSR tensors  $\mathbf{M}$  for the nuclei in the two enantiomers of a chiral molecule is expected to appear, but if the PV effects are neglected, the  $\mathbf{M}$  values of the two enantiomers will be equal. The difference appearing as a PV effect is due to an asymmetry in the electronic environments around the nuclei arising from weak interactions. As suggested by Barra *et al.*, PV effects will contribute not only to the NSR constants but also to the NMR shielding and indirect spin-spin coupling tensors [23]. An experimental observation of PV effects in one

\*Author to whom correspondence should be addressed.  
agustin.aucar@conicet.gov.ar

of these parameters would give rise to the first detection of PV interactions in a static system. Atomic experiments to detect weak interactions, in contrast, need transition phenomena [36].

In this paper we explore the PV effects on the NSR tensors of the central nuclei of tetrahedral chiral molecules, focusing on the role of the electronic environment and the central metal atom's atomic number. We use the relativistic theoretical formalism we recently derived [37] based on previous investigations into parity-conserving (PC) NSR tensors within the relativistic domain [38–40]. Furthermore, we report values of four-component (4C) isotropic PV nuclear shielding constants.

We analyze the W and U nuclei in the NWXYZ and NUXYZ series of molecules, respectively (with  $X, Y, Z = \text{H, F, Cl, Br, and I}$ ), and also the  $X$  nuclei in the NXHFZ molecules ( $X = \text{Cr, Se, Mo, Te, and Po}$  and  $Z = \text{Cl, Br, and I}$ ). Some of the chosen systems have been used previously to investigate PV effects on NMR shieldings and other molecular properties [41–44].

We present a systematic analysis of relativistic and electronic correlation effects on the PV NSR and PV shielding tensors, employing the polarization propagator theory to calculate the corresponding linear response functions within the random-phase approximation (RPA) theory based on the Dirac-Coulomb (DC) Hamiltonian. The Dirac-Hartree-Fock (DHF) and Dirac-Kohn-Sham (DKS) methodologies were used to obtain the wave functions. In order to compare relativistic 4C calculations with their non-relativistic (NR) limit, we also employed the Lévy-Leblond (LL) Hamiltonian.

This work has the following structure. In Sec. II we give a brief theoretical background to introduce the relativistic formulation used to calculate the NSD PV NSR and NSD PV shielding tensors. In Sec. III we provide the computational details for all the calculations presented in this paper, divided into two main parts, geometry optimizations and linear response calculations, including a short analysis of the basis-set convergence of the PV NSR constants in one of the studied molecules. In Sec. IV we present the 4C computations of the isotropic NSD PV NSR and NSD PV shielding constants for all the molecules studied here. The relativistic and electronic correlation effects are studied in this section, as well as the influence of different ligands (keeping the same metal nucleus or chiral center) and different chiral centers for the same ligand. Section V contains a summary and conclusions as well as an outlook for future work.

## II. THEORY

Within the polarization propagator theory, any static (i.e., zero-frequency) second-order molecular property can be calculated as [45,46]

$$E_{PQ}^{(2)} = \text{Re}[\langle\langle \hat{H}^P; \hat{H}^Q \rangle\rangle_{\omega=0}], \quad (1)$$

where the operators  $\hat{H}^P$  and  $\hat{H}^Q$  are any perturbative Hamiltonians. The linear response function on the right-hand side of Eq. (1) can also be written as the product of the perturbator  $\mathbf{b}^P$  (i.e., the property matrix element), the principal propagator  $\mathbf{M}^{-1}$  (i.e., the inverse of the electronic Hessian), and the perturbator  $\mathbf{b}^Q$  [37,47]. The linear response function

is usually computed by solving the response equation

$$\mathbf{M}\mathbf{X}^Q(\omega) = \mathbf{b}^Q, \quad (2)$$

where  $\mathbf{X}^Q(\omega) = \mathbf{M}^{-1}\mathbf{b}^Q$  is expanded into a linear combination of trial vectors and then contracted with the property matrix  $\mathbf{b}^P$  [48].

In the particular case of the nuclear spin-rotation and the NMR shielding tensors of a nucleus  $N$  ( $\mathbf{M}_N$  and  $\sigma_N$ , respectively), it is known that they can be obtained as the second-order energy derivatives at zero frequency [38,49]

$$\mathbf{M}_N = -\hbar \left. \frac{\partial^2 E(\mathbf{I}_N, \mathbf{J})}{\partial \mathbf{I}_N \partial \mathbf{J}} \right|_{\mathbf{I}_N=\mathbf{J}=0}, \quad (3)$$

$$\sigma_N = \left. \frac{\partial^2 E(\boldsymbol{\mu}_N, \mathbf{B}_0)}{\partial \boldsymbol{\mu}_N \partial \mathbf{B}_0} \right|_{\boldsymbol{\mu}_N=\mathbf{B}_0=0}, \quad (4)$$

where  $\hbar = \frac{h}{2\pi}$  is the reduced Planck constant,  $\mathbf{I}_N$  is the dimensionless spin of nucleus  $N$ ,  $\mathbf{J}$  is the molecular rotational angular momentum around the molecular center of mass (c.m.),  $\mathbf{B}_0$  is a uniform external magnetic field, and  $\boldsymbol{\mu}_N = \gamma_N \hbar \mathbf{I}_N$  is the magnetic moment due to the nuclear spin, where  $\gamma_N = \frac{e}{2m_p} g_N$  is the gyromagnetic ratio of nucleus  $N$  and  $g_N$  is its  $g$  factor, with  $e$  the fundamental charge and  $m_p$  the proton mass. The NSR tensor  $\mathbf{M}_N$  in Eq. (3) is given in units of energy. Therefore, by dividing it by the Planck constant  $h$ , the corresponding frequency values are obtained. SI units are used in the present work.

The NSD PV contribution to the NSR tensor has recently been derived within a relativistic framework and it has been demonstrated that it can be written as the linear response function [37]

$$\mathbf{M}_N^{\text{PV}} = \frac{\hbar G_F}{2\sqrt{2}c_0} \kappa_N \langle\langle \rho_N(\mathbf{r}) c \boldsymbol{\alpha}; \mathbf{J}_e \rangle\rangle \cdot \mathbf{I}^{-1}, \quad (5)$$

where  $G_F$  is the Fermi coupling constant, whose most recent value is  $G_F/(\hbar c_0)^3 = 1.1663787 \times 10^{-5} \text{ GeV}^{-2}$ , or equivalently  $G_F \simeq 2.222516 \times 10^{-14} E_h a_0^3$  [50]. In addition,  $\kappa_N = -2\lambda_N(1 - 4\sin^2\theta_W)$ , where  $\lambda_N$  is a nuclear state-dependent parameter. Note that the constant factor in the NSD PV Hamiltonian is found to be written in different ways in the literature [22,23,25,32,37,44,51,52]. There are three predominant contributions to  $\lambda_N$  due to the following interactions [53,54]: the weak coupling between neutral electronic vectors and nucleon axial-vector currents [55], the electromagnetic interactions between electrons and nuclear anapole moments (which become the dominant contributions for heavy nuclei) [56–58], and the nuclear-spin-independent electron axial vector and nucleon vector current weak interactions combined with hyperfine interactions [59].

As  $\lambda_N$  is a factor with a nuclear structure origin and to facilitate the comparison with previous works, we set  $\lambda_N = 1$  in our calculations. Therefore, all the reported values of  $\mathbf{M}_N^{\text{PV}}$  and  $\sigma_N^{\text{PV}}$  must be scaled by the true value of  $\lambda_N$  in order to get results that can be compared with measurable physical quantities. For heavy nuclei, it is expected that  $1 < \lambda_N < 10$  [56,57].

While the most recent value of the sine-squared weak mixing angle  $\theta_W$  is 0.23857(5) [60], we use  $\sin^2\theta_W = 0.2319$  [61] as the Weinberg parameter throughout this work for ease of comparison with earlier investigations [37]. In addition, in

Eq. (5)  $\alpha$  are the  $4 \times 4$  Dirac matrices given in the standard representation based on the Pauli spin matrices;  $\mathbf{r}$  is the position of the electrons with respect to the coordinate origin;  $\rho_N(\mathbf{r})$  is the normalized nuclear electric charge density of the nucleus  $N$  at the position of the electron (given in units of the inverse of cube distances);  $\frac{1}{c_0}$  is linearly proportional to the fine-structure constant (in SI units, the fine-structure constant is  $\frac{1}{4\pi\epsilon_0} \frac{e^2}{\hbar c_0}$ );  $c$  is the speed of light in vacuum, scalable to infinity at the NR limit;  $\mathbf{I}^{-1}$  is the inverse molecular inertia tensor with respect to the molecular c.m. in the equilibrium geometry; and  $\mathbf{J}_e = \mathbf{L}_e + \mathbf{S}_e$  is the  $4 \times 4$  total electronic angular momentum operator.

In the present work we neglect the contributions to Eq. (5) due to the Breit electron-nucleus interaction. These were shown to be very small for the PC NSR tensors [40].

Similarly to Eq. (5), the NSD PV contribution to the NMR shielding tensor is given by [25,31]

$$\sigma_N^{\text{PV}} = \frac{m_p G_F}{2\sqrt{2}\hbar c_0} \frac{\kappa_N}{g_N} \langle\langle \rho_N(\mathbf{r}) c \alpha; \mathbf{r}_{\text{GO}} \times c \alpha \rangle\rangle, \quad (6)$$

where  $\mathbf{r}_{\text{GO}} = \mathbf{r} - \mathbf{R}_{\text{GO}}$  is the electronic position relative to the gauge origin position for the external magnetic potential. The NR limits for the PV NSR and PV NMR shielding tensors given in Eqs. (5) and (6), respectively, were derived by some of us in Ref. [37] by applying the linear response within the elimination of small components (LRESC) approach. In the same work it was shown that the NR limits of the linear response functions involved in Eqs. (5) and (6) are exactly equal to each other in the cases where  $\mathbf{R}_{\text{GO}}$  is placed at the molecular c.m. Following the LRESC model [38,62,63], it is possible to expand these two relativistic second-order properties in terms of the fine-structure constant and to get their leading-order relativistic corrections. In this way, it can be shown that a close relationship between these properties also appears in the relativistic regime [64].

When the two enantiomers of a chiral molecule are analyzed, the isotropic NSR constants  $M_{X,\text{iso}} = \frac{1}{3} \text{Tr}(\mathbf{M}_X)$  of their chiral centers  $X$  will be given as the sum of a PC and a PV contribution  $M_{X,\text{iso}} = M_{X,\text{iso}}^{\text{PC}} \pm M_{X,\text{iso}}^{\text{PV}}$ , where the PV term of each of the two enantiomers has the opposite sign with respect to the other. This means that there will be a difference between the isotropic NSR constants of the same nuclei in the left ( $S$ )- and right ( $R$ )-handed enantiomers  $|\Delta M_{X,\text{iso}}| = |M_{X,\text{iso}}^S - M_{X,\text{iso}}^R|$ , which will be given by

$$|\Delta M_{X,\text{iso}}| = 2 |M_{X,\text{iso}}^{\text{PV}}|. \quad (7)$$

Similarly, for the NMR shielding constants,

$$|g_X \Delta \sigma_{X,\text{iso}}| = 2 |g_X \sigma_{X,\text{iso}}^{\text{PV}}| \quad (8)$$

holds, where  $|\Delta \sigma_{X,\text{iso}}| = |\sigma_{X,\text{iso}}^S - \sigma_{X,\text{iso}}^R|$ . Therefore, the measured absolute value of the NMR frequency splitting of the nucleus  $X$  in a static homogeneous magnetic field of flux density  $B_0$  ( $\Delta \nu_X$ ) is

$$\begin{aligned} |\Delta \nu_X| &= |v_X^S - v_X^R| = \frac{B_0 |\gamma_X \sigma_{X,\text{iso}}^{\text{PV}}|}{\pi} \\ &= B_0 \frac{e}{4\pi m_p} |g_X \Delta \sigma_{X,\text{iso}}|. \end{aligned} \quad (9)$$

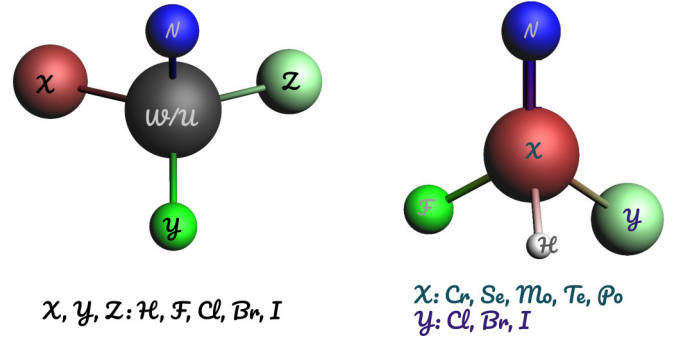


FIG. 1. Schematic representation of the molecules studied in this work.

In the following, we will report the quantities  $|\Delta M_{X,\text{iso}}|$  and  $|g_X \Delta \sigma_{X,\text{iso}}|$ .

### III. COMPUTATIONAL DETAILS

In this work we study the PV NSR and PV NMR shielding tensors of the  $^{183}\text{W}$  and  $^{235}\text{U}$  nuclei in the NWXYZ and NUXYZ series of molecules (with  $X, Y, Z = {}^1\text{H}, {}^{19}\text{F}, {}^{35}\text{Cl}, {}^{79}\text{Br}$ , and  $^{127}\text{I}$ ), as well as in the  $X$  nuclei in the NXHFZ systems (with  $X = {}^{53}\text{Cr}, {}^{77}\text{Se}, {}^{95}\text{Mo}, {}^{125}\text{Te}$ , and  $^{209}\text{Po}$  and  $Z = {}^{35}\text{Cl}, {}^{79}\text{Br}$ , and  $^{127}\text{I}$ ), which are schematically shown in Fig. 1. This selection of molecules allows us to analyze the effects produced by both the ligands and the chiral centers on the studied properties.

We optimized all the molecular geometries using density functional theory (DFT) with the PBE0 functional, which mixes the parameter-free Perdew-Burke-Ernzerhof (PBE) and Hartree-Fock exchange energies, along with the full PBE correlation energy [65]. Furthermore, we used scalar relativistic pseudopotentials for the Se, Br, Mo, Te, I, W, Po, and U heavy elements [66–68]. The aug-cc-pV5Z basis sets were used on the H, N, F [69,70], Cl [71], and Cr [72] light elements, whereas the aug-cc-pV5Z-PP basis sets were employed for the heavy atoms Se, Br [73], Mo [74], Te, I [73,75], W [76], and Po [73]. Since the aug-cc-pV5Z-PP basis sets are not available for U, for this element we used the atomic natural orbital valence basis set along with the Stuttgart pseudopotentials [77–79]. The obtained structural parameters are shown in the Supplemental Material [80]. All the optimizations were performed using the default settings in the energy minimization scheme of the GAUSSIAN program package [81].

Regarding the parity-violation contributions to the properties analyzed in this work, to calculate  $\sigma^{\text{PV}}$  we used the DIRAC program package [82,83], whereas to obtain the values of  $\mathbf{M}^{\text{PV}}$  we employed a locally modified version of the same code. We used the DC and the LL Hamiltonians to obtain the relativistic and the NR results, respectively [84], following the standard procedure in the DIRAC code to avoid the explicit calculation of the  $\langle SS|SS \rangle$  integrals [85].

Unless otherwise stated, we have employed the dyall.cv3z basis sets for all the elements studied in this work [86–93] and the small-component basis sets were generated from the large-component basis sets in all cases by applying the unrestricted kinetic balance prescription [94]. For the tungsten nucleus in

TABLE I.  $M_{\text{iso}}^{\text{PV}}$  (in  $\mu\text{Hz}$ ) for the  $^{183}\text{W}$  nucleus in the NWHFI molecule for different Dyall basis sets, using the DC Hamiltonian and the DFT PBE0 approach.

$X$	dyall.vXz	dyall.cvXz	dyall.aeXz
2	33.29	33.40	33.40
3	34.80	34.88	34.89
4	35.02	35.07	35.08

the NWHFI molecule, an analysis of the basis set convergence of  $M_{\text{iso}}^{\text{PV}}$  was performed. In Table I we present the results of our calculations using the dyall.vYz, dyall.cvYz, and dyall.aeYz basis sets, with  $Y = 2, 3,$  and  $4$  [86–88,91,93,95,96]. Since the value obtained using the dyall.cv3z basis set exhibits good convergence, this is the basis set we use throughout this work.

The gauge origin for the external magnetic potential has been placed at the molecular c.m. Furthermore, a spherically symmetric Gaussian-type nuclear charge density distribution model was used [97], as it has been shown that use of a finite nuclear model is important to adequately describe the PC NSR and PC NMR shielding tensors [98,99]. The nuclear  $g$  factors that were used to calculate  $\sigma_N^{\text{PV}}$  were taken from Ref. [100] and their values are displayed in Table II.

The response calculations were carried out at the 4C RPA level of theory employing the DHF and DKS DFT wave functions. In the DFT calculations, we used the NR exchange-correlation hybrid PBE0 functional because of its good performance in the 4C calculations of PC NSR constants (in comparison with experimental values) [98,101].

A deeper analysis of the electronic correlation effects was performed for the NXHFZ series of molecules (with  $X = \text{W}$  and  $\text{U}$  and  $Z = \text{Cl}, \text{Br},$  and  $\text{I}$ ). For these systems, we calculated  $M_{X,\text{iso}}^{\text{PV}}$  and  $\sigma_{X,\text{iso}}^{\text{PV}}$  using the LDA [102,103], PBE [104], PBE0 [65], and Coulomb attenuated method (CAM)-B3LYP [105] DFT functionals. The response of Eq. (2) was solved with respect to the property gradient associated with the following operators: (i) The total electronic orbital and spin angular momenta operators, to calculate  $M^{\text{PV}}$ , and (ii) the external magnetic field, for  $\sigma^{\text{PV}}$ .

#### IV. RESULTS AND DISCUSSION

We report 4C relativistic calculations of isotropic PV NSR and PV NMR shielding constants. These linear response properties are obtained by applying the RPA approach from the polarization propagator theory, combined with DHF and DKS

TABLE II. Nuclear  $g$  factors used to calculate  $\sigma_X^{\text{PV}}$ .

$X$	$g_X$
$^{53}\text{Cr}$	−0.31636
$^{77}\text{Se}$	1.070084
$^{95}\text{Mo}$	−0.36568
$^{125}\text{Te}$	−1.77701
$^{183}\text{W}$	0.235569
$^{209}\text{Po}$	1.376
$^{235}\text{U}$	−0.1085714286

wave functions based on the DC Hamiltonian. The influence of electron correlation effects (taken as the difference between linear response calculations using DKS and DHF wave functions) as well as of relativistic effects on the calculated properties is investigated. We then proceed to analyze the effects of the chiral center and of the chemical environment. These topics are addressed separately in the following sections.

#### A. Correlation and relativistic effects

In this section we investigate the effects of relativity and electron correlation in the calculations of  $M_{\text{U,iso}}^{\text{PV}}$  and  $\sigma_{\text{U,iso}}^{\text{PV}}$  for the NUHFZ series of molecules, with  $X = \text{Cl}, \text{Br},$  and  $\text{I}$ . We analyze the differences between the 4C and NR values, as well as between the DFT PBE0-based and the DHF-based calculations, in order to analyze both effects.

In Table III and Fig. 2(a), the inclusion of relativity and electronic correlation is seen to have the opposite effect. At the DHF RPA level of theory (4C RPA vs NR RPA), relativistic effects increase the values of  $|\Delta M_{\text{U,iso}}|$  significantly (with a 4C-to-NR ratio between 13 and 22). However, the calculated relativistic and NR values of  $|\Delta M_{\text{U,iso}}|$  are closer in magnitude when electron correlation is included using the DFT methodology (4C PBE0 vs NR PBE0), with a 4C-to-NR ratio of just between 5 and 7. The above observations demonstrate the importance of using a relativistic framework for meaningful investigations of these properties. Correlation effects are more pronounced in the relativistic regime than in the NR one. For  $|g_{\text{U}}\Delta\sigma_{\text{U,iso}}|$  [Fig. 2(b)], the effect of electron correlation is also to decrease the calculated values significantly. Therefore, reliable calculations of isotropic PV NSR and PV NMR shielding constants require the simultaneous inclusion of both relativistic and correlation effects. Instabilities of the Kramers restricted DHF and DKS wave functions appear in the LL calculations of  $\sigma_{\text{U,iso}}^{\text{PV}}$  and that is why they are not reported in this work.

We also evaluate the dependence of the calculated properties on the chosen functional at the 4C DFT level of theory. While  $|g_{\text{U}}\Delta\sigma_{\text{U,iso}}|$  remains stable as the DFT functional changes,  $|\Delta M_{\text{U,iso}}|$  varies significantly [see Figs. 2(a) and 2(b)].

Figures 3(a) and 3(b) show the relativistic effects at the DFT PBE0 level of theory in the calculations of  $M_{\text{iso}}^{\text{PV}}$  for the tungsten and uranium nuclei in the NWXYZ and NUXYZ systems (with  $X, Y, Z = \text{H}, \text{F}, \text{Cl}, \text{Br},$  and  $\text{I}$ ), respectively. The H- and F-containing systems exhibit the largest isotropic PV NSR constants in both the NR and 4C regimes. In Fig. 4, a similar behavior can be observed for  $g_{\text{W}}\sigma_{\text{W,iso}}^{\text{PV}}$  in the NWXYZ set of molecules (with  $X, Y, Z = \text{H}, \text{F}, \text{Cl}, \text{Br},$  and  $\text{I}$ ).

#### B. Fixing chiral centers: Analysis of the environment

We first focus our analysis on how the ligands affect the calculated values of  $|\Delta M_{K,\text{iso}}|$  and  $|g_K\Delta\sigma_{K,\text{iso}}|$  in the NKXYZ series of molecules (with  $K = \text{W}$  and  $\text{U}$  and  $X, Y, Z = \text{H}, \text{F}, \text{Cl}, \text{Br},$  and  $\text{I}$ ), as shown in Table IV.

In Fig. 5 we have classified all the systems into three different groups: (i) Systems containing both H and F atoms, (ii) Systems containing only H atoms without fluorine, and

TABLE III. Isotropic shifts of PV NSR and PV NMR shielding constants ( $2|M_{U,iso}^{PV}|$ , in  $\mu\text{Hz}$ , and  $2|g_U\sigma_{U,iso}^{PV}|$ , in  $\mu\text{ppm}$ , respectively) for the  $^{235}\text{U}$  nucleus in the NUHFX ( $X = \text{Cl, Br, and I}$ ) set of molecules, using different methods

Hamiltonian	Method	$2 M_{U,iso}^{PV} $			$2 g_U\sigma_{U,iso}^{PV} $		
		$X = \text{Cl}$	$X = \text{Br}$	$X = \text{I}$	$X = \text{Cl}$	$X = \text{Br}$	$X = \text{I}$
LL (NR)	DHF RPA	28.4	35.0	41.8			
LL (NR)	DFT PBE0	23.4	21.6	26.4			
DC (4C)	DHF RPA	604.0	652.0	542.0	67.4	80.2	65.7
DC (4C)	DFT LDA	200.0	240.0	220.0	0.8	0.7	1.8
DC (4C)	DFT PBE	196.6	238.0	214.0	0.7	0.0	0.4
DC (4C)	DFT CAMB3LYP	99.8	117.4	119.2	4.4	4.9	5.8
DC (4C)	DFT PBE0	121.4	142.6	141.0	2.8	3.5	5.4

(iii) Systems containing no H atoms. In Fig. 5(a) it is seen that the size of  $|\Delta M_{K,iso}|$  (with  $K = \text{W}$  and  $\text{U}$ ) follows (i) > (ii) > (iii).

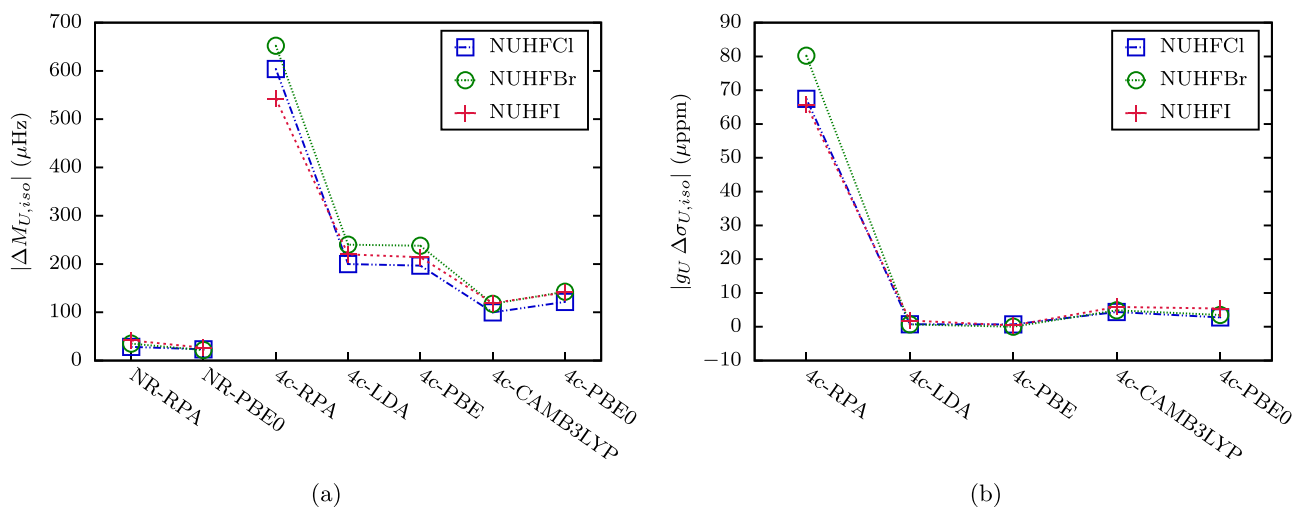
As stated in Sec. IV A, the systems containing H and F have the largest isotropic PV NSR constants. This can be due to

 TABLE IV. Calculations of  $2|M_{K,iso}^{PV}|$  (in  $\mu\text{Hz}$ ) and  $2|g_K\sigma_{K,iso}^{PV}|$  (in  $\mu\text{ppm}$ ) for the  $K = ^{183}\text{W}$  and  $^{235}\text{U}$  nuclei in the NKXYZ series of molecules (with  $X, Y, Z = \text{H, F, Cl, Br, and I}$ ). The DC Hamiltonian was used at the DFT PBE0 level of approach.

XYZ	$2 M_{K,iso}^{PV} $ ( $\mu\text{Hz}$ )		$2 g_K\sigma_{K,iso}^{PV} $ ( $\mu\text{ppm}$ )	
	$K = \text{W}$	$K = \text{U}$	$K = \text{W}$	$K = \text{U}$
HFCI	50.40	121.40	0.93	2.77
HFBBr	62.40	142.60	1.66	3.48
HFI	69.80	141.00	3.26	5.40
HCIBr	7.70	25.80	0.77	0.84
HClI	15.74	42.20	2.50	3.66
HBrI	0.90	12.56	1.73	2.54
FCIBr	4.10	4.36	0.08	0.38
FCII	4.24	1.79	0.19	0.81
FBrI	0.67	6.90	0.10	0.31
ClBrI	1.08	3.52	0.00	0.06

the fact that an increasingly asymmetric electronic distribution appears in the molecular chiral center when the difference in electronegativities between two of the ligands also increases. The electronegativities of the ligand atoms considered in this work follow the tendency  $\chi_{\text{F}} > \chi_{\text{Cl}} > \chi_{\text{Br}} > \chi_{\text{I}} > \chi_{\text{H}}$ . This implies that F and H have the largest and smallest electronegativities, respectively. On the other hand, a weaker cloud asymmetry at the chiral center may be the cause of the smallest PV effects seen in systems without H atoms. Additionally, since Cl and Br have comparable electronegativities, their coexistence will not result in a strong electron cloud asymmetry at the location of the chiral center, making the resulting PV effects some of the least significant in the group of molecules under study. This occurs despite the fact that molecules with Cl and Br are heavier than those with H and F.

As seen in Fig. 5(b),  $\sigma_{K,iso}^{PV}$  does not follow the same tendency. For  $|g_K\Delta\sigma_{K,iso}|$ , groups (i) and (ii) show more similar behavior, while the systems that do not contain hydrogen atoms [i.e., those of group (iii)] still yield the lowest values. The effect of the environment is remarkably large for these properties and more significant than the chiral center's atomic number in many cases. For instance,  $|\Delta M_{iso}|$  is much larger for tungsten in NWHFI than for uranium in the heavier NUCIBrI molecule. Therefore, we can identify the H- and


 FIG. 2. Calculated values of (a)  $|\Delta M_{U,iso}| = 2|M_{U,iso}^{PV}|$  (in  $\mu\text{Hz}$ ) and (b)  $|g_U\Delta\sigma_{U,iso}| = 2|g_U\sigma_{U,iso}^{PV}|$  (in  $\mu\text{ppm}$ ) for  $^{235}\text{U}$  in NUHFX molecular systems (with  $X = \text{Cl, Br, and I}$ ) employing the LL and DC Hamiltonians at the DHF, LDA, PBE, CAMB3LYP, and PBE0 levels of approach using the dyall.cv3z basis set for all elements.

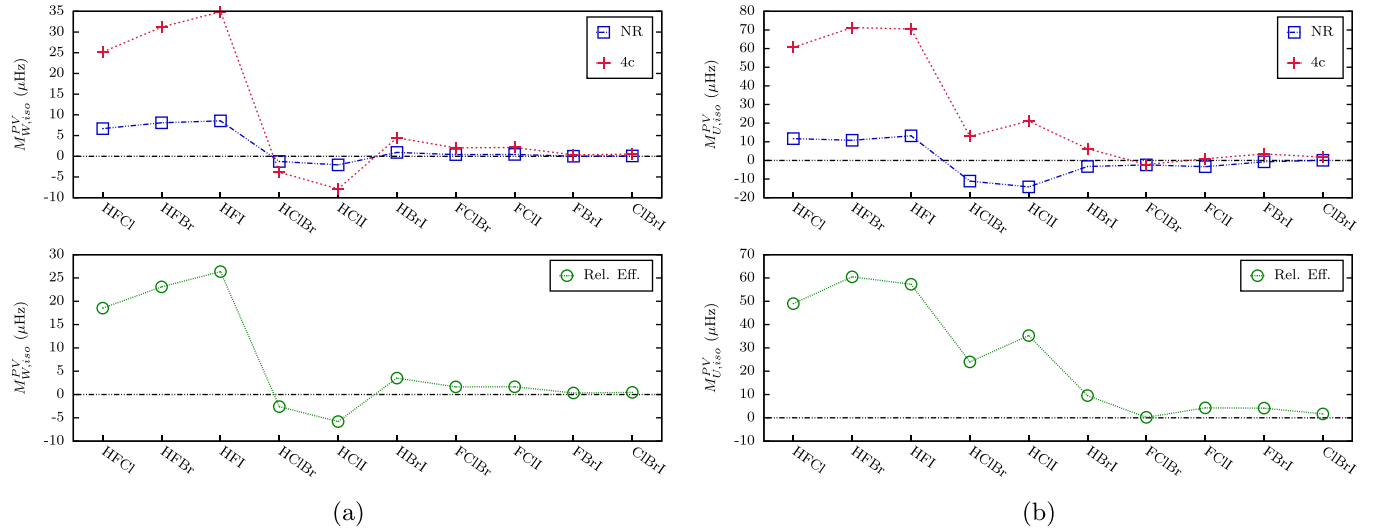


FIG. 3. Shown on top are the calculated values of  $M_{\text{iso}}^{\text{PV}}$  for (a)  $^{183}\text{W}$  and (b)  $^{235}\text{U}$  in the NWXYZ and NUXYZ systems ( $X, Y, Z = \text{H, F, Cl, Br, and I}$ ), respectively, employing the LL and DC Hamiltonians at the DFT PBE0 level of theory and using the dyall.cv3z basis set for all elements. On the bottom are relativistic effects taken as the difference between the 4C and NR values of  $M_{\text{iso}}^{\text{PV}}$ . All values are in  $\mu\text{Hz}$ .

F-containing systems as the most promising candidates for measurements in the investigated series. An earlier paper that examined PV effects in the NMR shieldings of the NWXYZ compounds came to similar conclusions [44].

### C. Fixing environment: Analysis of chiral centers

In general, U-containing systems have larger PV NSR and PV NMR shielding constants than W-containing systems (for the same ligand environment). Furthermore, when the ligands differ from H and F, there is no significant effect produced by the chemical environment.

To analyze the effects produced by the PV interactions as a function of the chiral center's atomic number, we include in the study further molecules containing elements with six

valence electrons and classify our sample into two groups according to their metal valence open-shell orbitals: The  $p$ -group elements Se, Te, and Po ( $s^2 p^4$ ) and the transition metals Cr, Mo ( $d^5 s^1$ ), W ( $d^4 s^2$ ), and U ( $f^3 d^1 s^2$ ). The obtained results are displayed in Table V.

Figures 6 and 7 present the values of  $|\Delta M_{X,\text{iso}}|$  and  $|g_X \Delta \sigma_{X,\text{iso}}|$  for the  $X$  nuclei in NXHFY systems with  $X = {}^{53}\text{Cr}, {}^{77}\text{Se}, {}^{95}\text{Mo}, {}^{125}\text{Te}, {}^{183}\text{W}, {}^{209}\text{Po},$  and  $^{235}\text{U}$  and with  $Y = \text{Cl, Br, and I}$  as a function of the chiral center's atomic number, respectively. As expected, the PV NSR and PV NMR shielding constants increase with the atomic number. However, it is interesting to note that this dependence is different for the two groups of molecules. Generally, the PV NSR and PV NMR shieldings increase faster with the atomic number in the systems containing  $p$  open-shell orbitals than in those with  $d$  open shells. We found that the excitations from the valence shells contribute the most to these properties in the

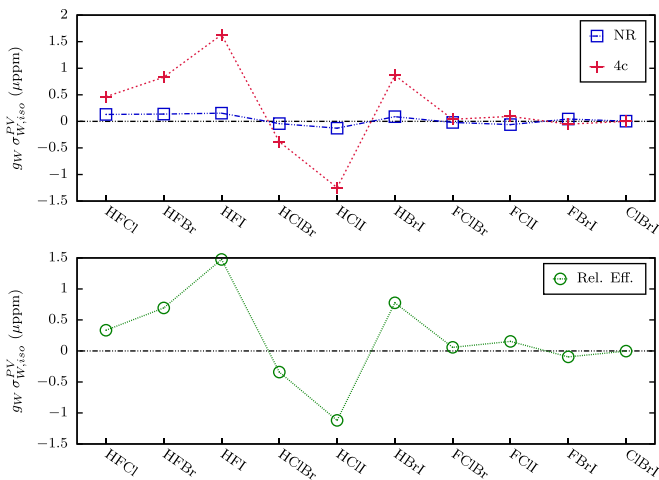


FIG. 4. Shown on top are the calculated values of  $g_W \sigma_{W,\text{iso}}^{\text{PV}}$  for the  $^{183}\text{W}$  nucleus in the NWXYZ systems ( $X, Y, Z = \text{H, F, Cl, Br, and I}$ ), employing the LL and DC Hamiltonians at the DFT PBE0 level of theory and using the dyall.cv3z basis set for all elements. On the bottom are relativistic effects taken as the difference between the 4C and NR values of  $g_W \sigma_{W,\text{iso}}^{\text{PV}}$ . All values are given in  $\mu\text{ppm}$ .

TABLE V. Calculations of  $2|M_{K,\text{iso}}^{\text{PV}}|$  (in  $\mu\text{Hz}$ ) and  $2|g_K \sigma_{K,\text{iso}}^{\text{PV}}|$  (in  $\mu\text{ppm}$ ) for the  $K$  nuclei (with  $K = \text{Cr, Se, Mo, Te, W, Po, and U}$ ) in the NKHFY series of molecules (with  $X = \text{Cl, Br, and I}$ ). The DC Hamiltonian was used in the calculations at the DFT PBE0 level of approach. The DFT PBE level was used for Po-containing molecules to avoid instabilities of the Kramers restricted DKS wave functions appearing in the DFT PBE0 calculations of these systems.

$K$	$2 M_{K,\text{iso}}^{\text{PV}} $ ( $\mu\text{Hz}$ )			$2 g_K \sigma_{K,\text{iso}}^{\text{PV}} $ ( $\mu\text{ppm}$ )		
	NKHFCI	NKHFBBr	NKHFI	NKHFCI	NKHFBBr	NKHFI
Cr	0.52	0.61	0.59	0.02	0.02	0.10
Se	6.34	9.76	10.40	0.08	0.08	0.04
Mo	6.18	7.96	8.86	0.09	0.20	0.47
Te	14.72	25.80	28.20	1.07	1.41	1.26
W	50.40	62.40	69.80	0.93	1.66	3.26
Po	286.00 <sup>a</sup>	478.00 <sup>a</sup>	600.00 <sup>a</sup>	3.94 <sup>a</sup>	3.26 <sup>a</sup>	10.34 <sup>a</sup>
U	121.40	142.60	141.00	2.77	3.48	5.40

<sup>a</sup>Calculated using the DFT PBE functional.

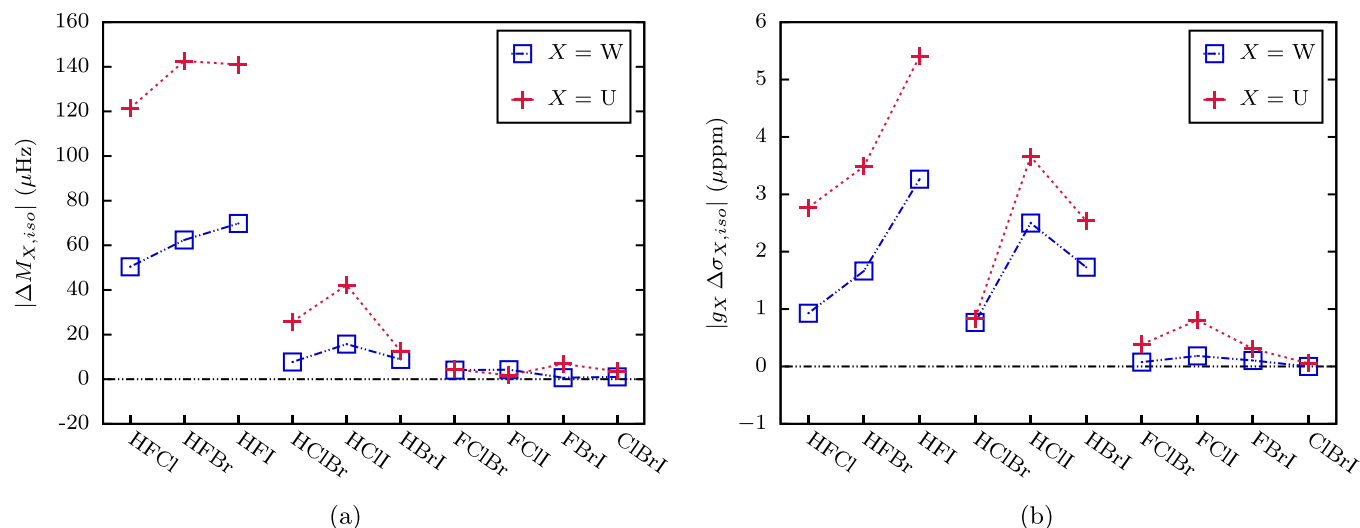


FIG. 5. Calculated values of (a)  $|\Delta M_{X,iso}| = 2|M_{X,iso}^{PV}|$  (in  $\mu\text{Hz}$ ) and (b)  $|g_X \Delta\sigma_{X,iso}| = 2|g_X \sigma_{X,iso}^{PV}|$  (in  $\mu\text{ppm}$ ) for the  $X$  nuclei (with  $X = W$  and  $U$ ) in molecules with different sets of ligands, employing the DC Hamiltonian at the DFT PBE0 level of theory and using the dyall.cv3z basis set for all the elements.

linear responses of Eqs. (5) and (6). We can thus explain the difference in the trends by the fact that the valence electrons in the  $p$  orbitals experience higher relativistic effects and contract more than those in  $d$  and  $f$  shells, bringing the electrons closer to the nucleus. This leads us to find the largest PV effects in Po-containing systems. Notice that we have included systems containing  $U$  (heavier than  $Po$ ) in our study.

On the other hand, Figs. 6(a)–6(c) and also Figs. 7(a)–7(c) show the same dependence of both properties on the metal’s atomic number when  $Y$  is varied in  $NXHFY$  molecules. There is only one exception to this tendency, for  $|g_{Se} \Delta\sigma_{Se,iso}|$  in  $NSeHF$ .

## V. CONCLUSION

In this work the NSD PV contributions to the NSR and NMR shielding tensors were obtained using the relativistic expression proposed in Ref. [37] for a series of light- and heavy-element-containing tetrahedral molecules. We

have shown that relativity plays a crucial role in describing the PV effects in these parameters for the chiral centers of the  $NXYZ$  series of molecules (with  $A = Cr, Mo, W, Se, Te, Po,$  and  $U$  and  $X, Y, Z = H, F, Cl, Br,$  and  $I$ ). Electron correlation effects are as important as relativity for describing the PV NSR and PV NMR shielding constants in these molecules and are more pronounced in relativistic calculations than in NR calculations. Therefore, reliable calculations of  $M_{iso}^{PV}$  and  $\sigma_{iso}^{PV}$  require the simultaneous inclusion of both relativistic and correlation effects.

We have shown that molecules containing both  $H$  and  $F$  atoms exhibit the largest isotropic PV NSR and PV NMR shielding constants, making this choice of ligand the most promising for such investigations. Additionally, we provided a study of the effects produced by using different chiral centers while keeping both the  $H$  and  $F$  ligands. Here we included further tetrahedral molecules containing elements with six valence electrons as chiral centers. The isotropic PV NSR and PV NMR shielding constants increase with the chiral center’s atomic number. However, depending on

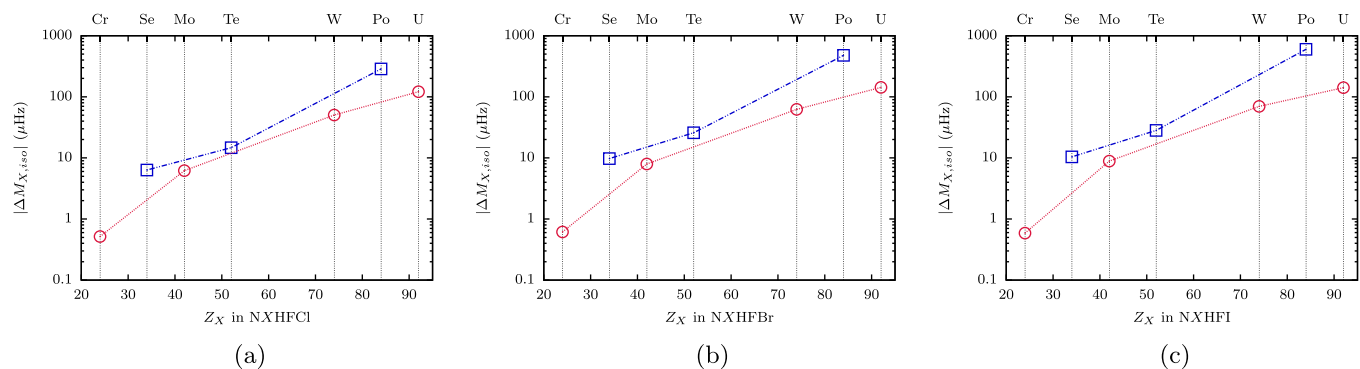


FIG. 6. Calculated values of  $|\Delta M_{X,iso}| = 2|M_{X,iso}^{PV}|$  (in  $\mu\text{Hz}$ ) for the  $X$  nuclei in the  $NXHFY$  systems, with  $X = Cr, Se, Mo, Te, W, Po,$  and  $U$  and for (a)  $Y = Cl$ , (b)  $Y = Br$ , and (c)  $Y = I$ , employing the DC Hamiltonian at the DFT PBE0 level of theory (except for  $X = Po$ , where the DFT PBE functional was used instead) and using the dyall.cv3z basis set for all the elements.

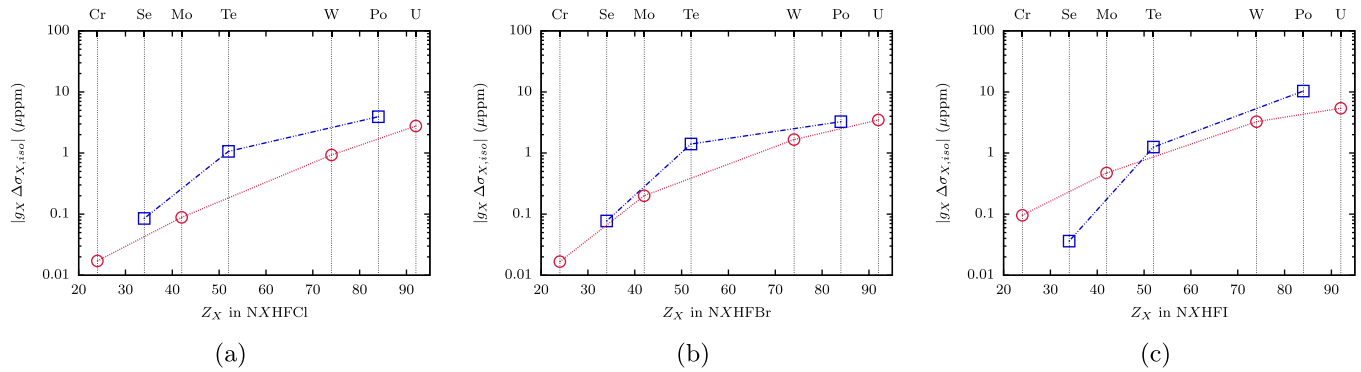


FIG. 7. Calculated values of  $|g_X \Delta\sigma_{X,\text{iso}}| = 2 |g_X \sigma_{X,\text{iso}}^{\text{PV}}|$  (in  $\mu\text{ppm}$ ) for the  $X$  nuclei in the NXHFY systems, with  $X = \text{Cr, Se, Mo, Te, W, Po, and U}$  and for (a)  $Y = \text{Cl}$ , (b)  $Y = \text{Br}$ , and (c)  $Y = \text{I}$ , employing the DC Hamiltonian at the DFT PBE0 level of theory (except for  $X = \text{Po}$ , where the DFT PBE functional was used instead) and using the dyall.cv3z basis set for all the elements.

the electronic structure of the metal atom, different tendencies emerge, that is, the PV NSR and PV NMR shielding constants increase faster with the atomic number in systems containing  $p$  open-shell orbitals than in those with  $d$  open shells.

We found the largest value of the NSR constant shift for the  $^{209}\text{Po}$  nucleus in NPoHFI, on the order of 0.6 mHz. While the PV NSR constants presented in this paper do not reach the experimental sensitivity limit for NSR constants, which is on the order of 1–10 Hz [106,107], this work provides important insights into a possible direction in the experimental search for PV effects in chiral molecules. The same molecule was also found to have the largest value of the PV NMR shielding constants calculated in this work. At a magnetic flux density of  $B_0 = 20$  T [see Eq. (9)], such as that used in Ref. [33], its NMR frequency splitting would reach 1.6 mHz, just about an order of magnitude below the projected sensitivity [33]. The prospects for detection of these effects in NMR spectroscopy seem favorable, provided a system with larger effects can be identified. A natural extension of this work is to search for promising molecules for measurements that are both experimentally accessible and benefit from larger PV contributions. The insights from this and previous studies on PV NMR shielding constants [33,44,108–112] can be used

as a starting point to identify new molecular candidates for further computational investigations.

## ACKNOWLEDGMENTS

This work was performed under Project HPC-EUROPA3 (No. INFRAIA-2016-1-730897), with the support of the EC Research Innovation Action under the H2020 Programme. In particular, I.A.A. gratefully acknowledges support from the University of Groningen, as well as computer resources and technical support provided by SURFsara. He also acknowledges partial support from FONCYT through Grants No. PICT-2016-2936 and No. PICT-2020-SerieA-00052. We would also like to thank the Institute for Modeling and Innovation in Technologies and the University of Groningen's Center for Information Technology for their support and for providing access to the IMIT and Peregrine high-performance computing clusters. This work also made use of the Dutch national e-infrastructure with the support of the SURF Cooperative using Grant No. EINF-3247. This publication is part of the project High sector Fock space coupled cluster method: Benchmark accuracy across the periodic table (through Project No. VI.Vidi.192.088 of the research program Vidi, which is financed by the Dutch Research Council).

- [1] T. D. Lee and C. N. Yang, Question of parity conservation in weak interactions, *Phys. Rev.* **104**, 254 (1956).
- [2] C. S. Wu, E. Ambler, R. W. Hayward, D. D. Hoppes, and R. P. Hudson, Experimental test of parity conservation in beta decay, *Phys. Rev.* **105**, 1413 (1957).
- [3] R. L. Garwin, L. M. Lederman, and M. Weinrich, Observations of the failure of conservation of parity and charge conjugation in meson decays: The magnetic moment of the free muon, *Phys. Rev.* **105**, 1415 (1957).
- [4] R. Conti, P. Bucksbaum, S. Chu, E. Commins, and L. Hunter, Preliminary Observation of Parity Nonconservation in Atomic Thallium, *Phys. Rev. Lett.* **42**, 343 (1979).
- [5] L. M. Barkov and M. S. Zolotarev, Parity nonconservation in bismuth atoms and neutral weak-interaction currents, *Zh. Eksp. Teor. Fiz.* **79**, 713 (1980) [*Sov. Phys. JETP* **52**, 360 (1980)].
- [6] M. A. Bouchiat, J. Guéna, L. Hunter, and L. Pottier, Observation of a parity violation in cesium, *Phys. Lett. B* **117**, 358 (1982).
- [7] T. P. Emmons, J. M. Reeves, and E. N. Fortson, Parity-Nonconserving Optical Rotation in Atomic Lead, *Phys. Rev. Lett.* **51**, 2089 (1983).
- [8] M. J. D. Macpherson, K. P. Zetie, R. B. Warrington, D. N. Stacey, and J. P. Hoare, Precise Measurement of Parity Nonconserving Optical Rotation at 876 nm in Atomic Bismuth, *Phys. Rev. Lett.* **67**, 2784 (1991).
- [9] C. S. Wood, S. C. Bennett, D. Cho, B. P. Masterson, J. L. Roberts, C. E. Tanner, and C. E. Wieman, Measurement of parity nonconservation and an anapole moment in cesium, *Science* **275**, 1759 (1997).
- [10] K. Tsigtukin, D. Dounas-Frazer, A. Family, J. E. Stalnaker, V. V. Yashchuk, and D. Budker, Observation of a Large



- Atomic Parity Violation Effect in Ytterbium, *Phys. Rev. Lett.* **103**, 071601 (2009).
- [11] M. A. Bouchiat, Atomic parity violation. Early days, present results, prospects, *Nuovo Cimento* **35**, 78 (2012).
- [12] V. S. Letokhov, On difference of energy levels of left and right molecules due to weak interactions, *Phys. Lett. A* **53**, 275 (1975).
- [13] O. Kompanets, A. Kukudzhanov, V. Letokhov, and L. Gervits, Narrow resonances of saturated absorption of the asymmetrical molecule CHFClBr and the possibility of weak current detection in molecular physics, *Opt. Commun.* **19**, 414 (1976).
- [14] A. Szabó-Nagy and L. Keszthelyi, Demonstration of the parity-violating energy difference between enantiomers, *Proc. Natl. Acad. Sci. USA* **96**, 4252 (1999).
- [15] R. Berger, in *Relativistic Electronic Structure Theory*, edited by P. Schwerdtfeger (Elsevier, Amsterdam, 2004), Vol. 14, pp. 188–288.
- [16] A. MacDermott and R. Hegstrom, A proposed experiment to measure the parity-violating energy difference between enantiomers from the optical rotation of chiral ammonia-like “cat” molecules, *Chem. Phys.* **305**, 55 (2004).
- [17] D. DeMille, S. B. Cahn, D. Murphree, D. A. Rahmlow, and M. G. Kozlov, Using Molecules to Measure Nuclear Spin-Dependent Parity Violation, *Phys. Rev. Lett.* **100**, 023003 (2008).
- [18] B. Darquié *et al.*, Progress toward the first observation of parity violation in chiral molecules by high-resolution laser spectroscopy, *Chirality* **22**, 870 (2010).
- [19] F. Hobi, R. Berger, and J. Stohner, Investigation of parity violation in nuclear spin-rotation interaction of fluorooxirane, *Mol. Phys.* **111**, 2345 (2013).
- [20] S. B. Cahn, J. Ammon, E. Kirilov, Y. V. Gurevich, D. Murphree, R. Paolino, D. A. Rahmlow, M. G. Kozlov, and D. DeMille, Zeeman-Tuned Rotational Level-Crossing Spectroscopy in a Diatomic Free Radical, *Phys. Rev. Lett.* **112**, 163002 (2014).
- [21] A. Cournol *et al.*, A new experiment to test parity symmetry in cold chiral molecules using vibrational spectroscopy, *Quantum Electron.* **49**, 288 (2019).
- [22] V. G. Gorshkov, M. G. Kozlov, and L. N. Labzovskii, P-odd effects in polyatomic molecules, *Zh. Eksp. Teor. Fiz.* **82**, 1807 (1982) [*Sov. Phys. JETP* **55**, 1042 (1982)].
- [23] A. L. Barra, J. B. Robert, and L. Wiesenfeld, Parity non-conservation and NMR observables. Calculation of TI resonance frequency differences in enantiomers, *Phys. Lett. A* **115**, 443 (1986).
- [24] A. Barra, J. Robert, and L. Wiesenfeld, Parity non conservation: NMR parameters in chiral molecules, *Biosystems* **20**, 57 (1987).
- [25] A. L. Barra, J. B. Robert, and L. Wiesenfeld, Possible observation of parity nonconservation by high-resolution NMR, *Europhys. Lett.* **5**, 217 (1988).
- [26] A. L. Barra and J. B. Robert, Parity non-conservation and NMR parameters, *Mol. Phys.* **88**, 875 (1996).
- [27] A. Soncini, F. Faglioni, and P. Lazzeretti, Parity-violating contributions to nuclear magnetic shielding, *Phys. Rev. A* **68**, 033402 (2003).
- [28] G. Laubender and R. Berger, Ab initio calculation of parity-violating chemical shifts in NMR spectra of chiral molecules, *Chem. Phys. Chem.* **4**, 395 (2003).
- [29] V. Weijs, P. Manninen, and J. Vaara, Perturbational calculations of parity-violating effects in nuclear-magnetic-resonance parameters, *J. Chem. Phys.* **123**, 054501 (2005).
- [30] G. Laubender and R. Berger, Electroweak quantum chemistry for nuclear-magnetic-resonance-shielding constants: Impact of electron correlation, *Phys. Rev. A* **74**, 032105 (2006).
- [31] R. Bast, P. Schwerdtfeger, and T. Saue, Parity nonconservation contribution to the nuclear magnetic resonance shielding constants of chiral molecules: A four-component relativistic study, *J. Chem. Phys.* **125**, 064504 (2006).
- [32] S. Nahrwold and R. Berger, Zeroth order regular approximation approach to parity violating nuclear magnetic resonance shielding tensors, *J. Chem. Phys.* **130**, 214101 (2009).
- [33] J. Eills, J. W. Blanchard, L. Bougas, M. G. Kozlov, A. Pines, and D. Budker, Measuring molecular parity nonconservation using nuclear-magnetic-resonance spectroscopy, *Phys. Rev. A* **96**, 042119 (2017).
- [34] J. W. Blanchard, J. P. King, T. F. Sjolander, M. G. Kozlov, and D. Budker, Molecular parity nonconservation in nuclear spin couplings, *Phys. Rev. Res.* **2**, 023258 (2020).
- [35] M. S. Safronova, D. Budker, D. DeMille, D. F. J. Kimball, A. Derevianko, and C. W. Clark, Search for new physics with atoms and molecules, *Rev. Mod. Phys.* **90**, 025008 (2018).
- [36] M.-A. Bouchiat and C. Bouchiat, Parity violation in atoms, *Rep. Prog. Phys.* **60**, 1351 (1997).
- [37] I. A. Aucar and A. Borschevsky, Relativistic study of parity-violating nuclear spin-rotation tensors, *J. Chem. Phys.* **155**, 134307 (2021).
- [38] I. A. Aucar, S. S. Gómez, M. C. Ruiz de Azúa, and C. G. Giribet, Theoretical study of the nuclear spin-molecular rotation coupling for relativistic electrons and non-relativistic nuclei, *J. Chem. Phys.* **136**, 204119 (2012).
- [39] I. A. Aucar, S. S. Gomez, J. I. Melo, C. G. Giribet, and M. C. Ruiz de Azúa, Theoretical study of the nuclear spin-molecular rotation coupling for relativistic electrons and non-relativistic nuclei. II. Quantitative results in HX (X = H, F, Cl, Br, I) compounds, *J. Chem. Phys.* **138**, 134107 (2013).
- [40] I. A. Aucar, S. S. Gómez, C. G. Giribet, and M. C. Ruiz de Azúa, Breit interaction effects in relativistic theory of the nuclear spin-rotation tensor, *J. Chem. Phys.* **139**, 094112 (2013).
- [41] D. Figgen, T. Saue, and P. Schwerdtfeger, Relativistic four- and two-component calculations of parity violation effects in chiral tungsten molecules of the form NWXYZ (X, Y, Z = H, F, Cl, Br, or I), *J. Chem. Phys.* **132**, 234310 (2010).
- [42] D. Figgen, A. Koers, and P. Schwerdtfeger, NWHCI: A small and compact chiral molecule with large parity-violation effects in the vibrational spectrum, *Angew. Chem. Int. Ed.* **49**, 2941 (2010).
- [43] M. Wormit, M. Olejniczak, A.-L. Deppenmeier, A. Borschevsky, T. Saue, and P. Schwerdtfeger, Strong enhancement of parity violation effects in chiral uranium compounds, *Phys. Chem. Chem. Phys.* **16**, 17043 (2014).
- [44] S. Nahrwold, R. Berger, and P. Schwerdtfeger, Parity violation in nuclear magnetic resonance frequencies of chiral tetrahedral tungsten complexes NWXYZ (X, Y, Z = H, F, Cl, Br or I), *J. Chem. Phys.* **140**, 024305 (2014).
- [45] J. Oddershede, in *Advances in Quantum Chemistry*, edited by P.-O. Löwdin (Academic, San Diego, 1978), Vol. 11, pp. 275–352.

- [46] G. A. Aucar, Toward a QFT-based theory of atomic and molecular properties, *Phys. Chem. Chem. Phys.* **16**, 4420 (2014).
- [47] G. A. Aucar, R. H. Romero, and A. F. Maldonado, Polarization propagators: A powerful theoretical tool for a deeper understanding of NMR spectroscopic parameters, *Int. Rev. Phys. Chem.* **29**, 1 (2010).
- [48] T. Saue and H. J. A. Jensen, Linear response at the 4-component relativistic level: Application to the frequency-dependent dipole polarizabilities of the coinage metal dimers, *J. Chem. Phys.* **118**, 522 (2003).
- [49] G. A. Aucar and I. A. Aucar, in *Annual Reports on NMR Spectroscopy*, edited by G. A. Webb (Academic, San Diego, 2019), Vol. 96, pp. 77–141.
- [50] E. Tiesinga, P. J. Mohr, D. B. Newell, and B. N. Taylor, *The 2018 CODATA Recommended Values of the Fundamental Physical Constants, Web Version 8.1*, <http://physics.nist.gov/constants>, database developed by J. Baker, M. Douma, and S. Kotochigova (National Institute of Standards and Technology, Gaithersburg, 2018).
- [51] A. Borschevsky, M. Iliaš, V. A. Dzuba, K. Beloy, V. V. Flambaum, and P. Schwerdtfeger,  $P$ -odd interaction constant  $W_A$  from relativistic *ab initio* calculations of diatomic molecules, *Phys. Rev. A* **85**, 052509 (2012).
- [52] T. A. Isaev and R. Berger, Electron correlation and nuclear charge dependence of parity-violating properties in open-shell diatomic molecules, *Phys. Rev. A* **86**, 062515 (2012).
- [53] I. B. Khriplovich, *Parity Nonconservation in Atomic Phenomena* (CRC, Boca Raton, 1991).
- [54] J. S. M. Ginges and V. V. Flambaum, Violations of fundamental symmetries in atoms and tests of unification theories of elementary particles, *Phys. Rep.* **397**, 63 (2004).
- [55] V. N. Novikov, O. P. Sushkov, V. V. Flambaum, and I. B. Khriplovich, Possibility of studying the structure of weak neutral currents in optical transitions in heavy atoms, *Zh. Eksp. Teor. Fiz.* **73**, 802 (1977) [*Sov. Phys. JETP* **46**, 420 (1977)].
- [56] V. V. Flambaum and I. Khriplovich,  $P$ -odd nuclear forces—A source of parity violation in atoms, *Zh. Eksp. Teor. Fiz.* **79**, 1656 (1980) [*Sov. Phys. JETP* **52**, 835 (1980)].
- [57] V. V. Flambaum, I. B. Khriplovich, and O. P. Sushkov, Nuclear anapole moments, *Phys. Lett. B* **146**, 367 (1984).
- [58] V. V. Flambaum and I. Khriplovich, On the enhancement of parity nonconserving effects in diatomic molecules, *Phys. Lett. A* **110**, 121 (1985).
- [59] V. V. Flambaum and I. B. Khriplovich, New bounds on the electric dipole moment of the electron and on  $T$ -odd electron-nucleon coupling, *Zh. Eksp. Teor. Fiz.* **89**, 1505 (1985) [*Sov. Phys. JETP* **62**, 872 (1985)].
- [60] P. A. Zyla *et al.* (Particle Data Group), Review of particle physics, *Prog. Theor. Exp. Phys.* **2020**, 083C01 (2020).
- [61] L. Montanet, K. Gieselmann, R. M. Barnett, D. E. Groom, T. G. Trippe, C. G. Wohl, B. Armstrong, G. S. Wagman, H. Murayama, J. Stone, J. J. Hernandez, F. C. Porter, R. J. Morrison, A. Manohar, M. Aguilar-Benitez, C. Caso, P. Lantero, R. L. Crawford, M. Roos, N. A. Tornqvist *et al.* (Particle Data Group), Review of particle properties, *Phys. Rev. D* **50**, 1173 (1994).
- [62] I. A. Aucar, S. S. Gomez, C. G. Giribet, and M. C. Ruiz de Azúa, Theoretical study of the relativistic molecular rotational  $g$ -tensor, *J. Chem. Phys.* **141**, 194103 (2014).
- [63] G. A. Aucar, J. I. Melo, I. A. Aucar, and A. F. Maldonado, Foundations of the LRESC model for response properties and some applications, *Int. J. Quantum Chem.* **118**, e25487 (2018).
- [64] I. A. Aucar, M. T. Colombo Jofré, and G. A. Aucar, Relativistic relationship between nuclear-spin-dependent parity-violating NMR shielding and nuclear spin-rotation tensors, [arXiv:2208.04788](https://arxiv.org/abs/2208.04788) [*Phys. Rev. A* (to be published)].
- [65] C. Adamo and V. Barone, Toward reliable density functional methods without adjustable parameters: The PBE0 model, *J. Chem. Phys.* **110**, 6158 (1999).
- [66] P. Pykkö, Relativistic effects in structural chemistry, *Chem. Rev.* **88**, 563 (1988).
- [67] J. Autschbach, Perspective: Relativistic effects, *J. Chem. Phys.* **136**, 150902 (2012).
- [68] P. Pykkö and S. Hermann, *Chemical Modelling: Applications and Theory* (Royal Society of Chemistry, London, 1999), Vol. 1.
- [69] T. H. Dunning, Gaussian basis sets for use in correlated molecular calculations. I. The atoms boron through neon and hydrogen, *J. Chem. Phys.* **90**, 1007 (1989).
- [70] R. A. Kendall, T. H. Dunning, and R. J. Harrison, Electron affinities of the first-row atoms revisited. Systematic basis sets and wave functions, *J. Chem. Phys.* **96**, 6796 (1992).
- [71] D. E. Woon and T. H. Dunning, Gaussian basis sets for use in correlated molecular calculations. III. The atoms aluminum through argon, *J. Chem. Phys.* **98**, 1358 (1993).
- [72] N. B. Balabanov and K. A. Peterson, Systematically convergent basis sets for transition metals. I. All-electron correlation consistent basis sets for the  $3d$  elements Sc–Zn, *J. Chem. Phys.* **123**, 064107 (2005).
- [73] K. A. Peterson, D. Figgen, E. Goll, H. Stoll, and M. Dolg, Systematically convergent basis sets with relativistic pseudopotentials. II. Small-core pseudopotentials and correlation consistent basis sets for the post- $d$  group 16–18 elements, *J. Chem. Phys.* **119**, 11113 (2003).
- [74] K. A. Peterson, D. Figgen, M. Dolg, and H. Stoll, Energy-consistent relativistic pseudopotentials and correlation consistent basis sets for the  $4d$  elements Y–Pd, *J. Chem. Phys.* **126**, 124101 (2007).
- [75] K. A. Peterson, B. C. Shepler, D. Figgen, and H. Stoll, On the spectroscopic and thermochemical properties of ClO, BrO, IO, and their anions, *J. Phys. Chem. A* **110**, 13877 (2006).
- [76] D. Figgen, K. A. Peterson, M. Dolg, and H. Stoll, Energy-consistent pseudopotentials and correlation consistent basis sets for the  $5d$  elements Hf–Pt, *J. Chem. Phys.* **130**, 164108 (2009).
- [77] X. Cao, M. Dolg, and H. Stoll, Valence basis sets for relativistic energy-consistent small-core actinide pseudopotentials, *J. Chem. Phys.* **118**, 487 (2003).
- [78] X. Cao and M. Dolg, Segmented contraction scheme for small-core actinide pseudopotential basis sets, *J. Mol. Struct. (THEOCHEM)* **673**, 203 (2004).
- [79] W. Küchle, M. Dolg, H. Stoll, and H. Preuss, Energy-adjusted pseudopotentials for the actinides. Parameter sets and test calculations for thorium and thorium monoxide, *J. Chem. Phys.* **100**, 7535 (1994).
- [80] See Supplemental Material at <http://link.aps.org/supplemental/10.1103/PhysRevA.106.062802> for the optimized structural parameters of the chiral molecules studied in this work.

- [81] M. J. Frisch *et al.*, *Gaussian 16, Revision C.01* (Gaussian Inc., Wallingford, 2016).
- [82] H. J. A. Jensen, R. Bast, A. S. P. Gomes, T. Saue, and L. Visscher, with contributions from I. A. Aucar, V. Bakken, C. Chibueze, J. Creutzberg, K. G. Dyall *et al.* DIRAC, a relativistic ab initio electronic structure program, Release DIRAC22 (2022), available at <http://dx.doi.org/10.5281/zenodo.6010450> (see also <http://www.diracprogram.org>).
- [83] T. Saue *et al.*, The DIRAC code for relativistic molecular calculations, *J. Chem. Phys.* **152**, 204104 (2020).
- [84] T. Saue, in *Advances in Quantum Chemistry*, edited by J. R. Sabin (Academic, San Diego, 2005), Vol. 48, pp. 383–405.
- [85] L. Visscher, Approximate molecular relativistic Dirac-Coulomb calculations using a simple Coulombic correction, *Theor. Chem. Acc.* **98**, 68 (1997).
- [86] K. G. Dyall, Relativistic and nonrelativistic finite nucleus optimized triple-zeta basis sets for the 4*p*, 5*p* and 6*p* elements, *Theor. Chem. Acc.* **108**, 335 (2002).
- [87] K. G. Dyall, Relativistic double-zeta, triple-zeta, and quadruple-zeta basis sets for the 5*d* elements Hf–Hg, *Theor. Chem. Acc.* **112**, 403 (2004).
- [88] K. G. Dyall, Relativistic quadruple-zeta and revised triple-zeta and double-zeta basis sets for the 4*p*, 5*p*, and 6*p* elements, *Theor. Chem. Acc.* **115**, 441 (2006).
- [89] K. G. Dyall, Relativistic double-zeta, triple-zeta, and quadruple-zeta basis sets for the 4*d* elements Y–Cd, *Theor. Chem. Acc.* **117**, 483 (2007).
- [90] K. G. Dyall, Relativistic double-zeta, triple-zeta, and quadruple-zeta basis sets for the actinides Ac–Lr, *Theor. Chem. Acc.* **117**, 491 (2007).
- [91] K. G. Dyall and A. S. P. Gomes, Revised relativistic basis sets for the 5*d* elements Hf–Hg, *Theor. Chem. Acc.* **125**, 97 (2010).
- [92] A. S. P. Gomes, K. G. Dyall, and L. Visscher, Relativistic double-zeta, triple-zeta, and quadruple-zeta basis sets for the lanthanides La–Lu, *Theor. Chem. Acc.* **127**, 369 (2010).
- [93] K. G. Dyall, Relativistic double-zeta, triple-zeta, and quadruple-zeta basis sets for the light elements H–Ar, *Theor. Chem. Acc.* **135**, 128 (2016).
- [94] G. A. Aucar, T. Saue, L. Visscher, and H. J. Aa. Jensen, On the origin and contribution of the diamagnetic term in four-component relativistic calculations of magnetic properties, *J. Chem. Phys.* **110**, 6208 (1999).
- [95] K. G. Dyall, Relativistic and nonrelativistic finite nucleus optimized double zeta basis sets for the 4*p*, 5*p* and 6*p* elements, *Theor. Chem. Acc.* **99**, 366 (1998).
- [96] K. G. Dyall, Core correlating basis functions for elements 31–118, *Theor. Chem. Acc.* **131**, 1217 (2012).
- [97] L. Visscher and K. G. Dyall, Dirac–Fock atomic electronic structure calculations using different nuclear charge distributions, *At. Data Nucl. Data Tables* **67**, 207 (1997).
- [98] I. A. Aucar, C. A. Giménez, and G. A. Aucar, Influence of the nuclear charge distribution and electron correlation effects on magnetic shieldings and spin-rotation tensors of linear molecules, *RSC Adv.* **8**, 20234 (2018).
- [99] A. F. Maldonado, C. A. Giménez, and G. A. Aucar, Nuclear charge-distribution effects on the NMR spectroscopy parameters, *J. Chem. Phys.* **136**, 224110 (2012).
- [100] P. Raghavan, Table of nuclear moments, *At. Data Nucl. Data Tables* **42**, 189 (1989).
- [101] D. F. E. Bajac, I. A. Aucar, and G. A. Aucar, Absolute NMR shielding scales in methyl halides obtained from experimental and calculated nuclear spin-rotation constants, *Phys. Rev. A* **104**, 012805 (2021).
- [102] S. J. Vosko, L. Wilk, and M. Nusair, Accurate spin-dependent electron liquid correlation energies for local spin density calculations: A critical analysis, *Can. J. Phys.* **58**, 1200 (1980).
- [103] P. Hohenberg and W. Kohn, Inhomogeneous electron gas, *Phys. Rev.* **136**, B864 (1964).
- [104] J. P. Perdew, K. Burke, and M. Ernzerhof, Generalized Gradient Approximation Made Simple, *Phys. Rev. Lett.* **77**, 3865 (1996).
- [105] T. Yanai, D. P. Tew, and N. C. Handy, A new hybrid exchange–correlation functional using the Coulomb-attenuating method (CAM-B3LYP), *Chem. Phys. Lett.* **393**, 51 (2004).
- [106] B. M. Giuliano, L. Bizzocchi, R. Sanchez, P. Villanueva, V. Cortijo, M. E. Sanz, and J.-U. Grabow, The rotational spectra, potential function, Born–Oppenheimer breakdown, and hyperfine structure of GeSe and GeTe, *J. Chem. Phys.* **135**, 084303 (2011).
- [107] J. H. Yoo, H. Köckert, J. C. Mullaney, S. L. Stephens, C. J. Evans, N. R. Walker, and R. J. Le Roy, Vibrational energies and full analytic potential energy functions of PbI and InI from pure microwave data, *J. Mol. Spectrosc.* **330**, 80 (2016).
- [108] R. Berger and J. L. Stuber, Electroweak interactions in chiral molecules: Two-component density functional theory study of vibrational frequency shifts in polyhalomethanes, *Mol. Phys.* **105**, 41 (2007).
- [109] R. Zanasi, S. Pelloni, and P. Lazzarotti, Chiral discrimination via nuclear magnetic shielding polarisabilities from NMR spectroscopy: Theoretical study of (*R<sub>a</sub>*)-1,3-dimethylallene, (2*R*)-2-methyloxirane, and (2*R*) – *N*-methyloxaziridine, *J. Comput. Chem.* **28**, 2159 (2007).
- [110] D. Figgen and P. Schwerdtfeger, SeOCII: A promising candidate for the detection of parity violation in chiral molecules, *Phys. Rev. A* **78**, 012511 (2008).
- [111] V. Weijs, P. Manninen, and J. Vaara, Effect of molecular size on the parity-non-conserving contributions to the nuclear magnetic resonance shielding constant, *Theor. Chem. Acc.* **121**, 53 (2008).
- [112] V. Weijs, M. B. Hansen, O. Christiansen, and P. Manninen, Vibrational effects in the parity-violating contributions to the isotropic nuclear magnetic resonance chemical shift, *Chem. Phys. Lett.* **470**, 166 (2009).